Viscous and Nonviscous Nonequilibrium Nozzle Flows

JEROME J. BRAINERD* AND ELY S. LEVINSKY†
General Dynamics/Astronautics, San Diego, Calif.

Two-dimensional or axially symmetric hypersonic gas flows with coupled, finite-rate chemical reactions are considered. The effects of reacting boundary layers over catalytic and noncatalytic walls are included. The equations of Wood and Kirkwood, with the simplifying assumption of local thermodynamic equilibrium, are integrated in a finite-difference procedure for the inviscid flow fields. The boundary-layer formulation is similar to that of Fay and Riddell, Lees, and Scala, except that local similarity is assumed over the full length of the surface being considered, and several chemical species may be considered. Both catalytic and noncatalytic wall effects are considered. Sample calculations are carried out for air (five chemical species), using Wray's reaction rates, for the flow in a hypersonic nozzle with boundary layer.

Nomenclature

A_j^f, A_j^r = coefficients of the forward and reverse rate constants, jth reaction
a = spacing of points along data line, inviscid calculation
b = step size, inviscid calculation
C_i = mass fraction, ith species
C_p^0 = frozen specific heat at constant pressure
c_0 = frozen speed of sound
D_i = binary diffusion coefficient, ith species
E_j^f, E_j^r = forward and reverse activation energies, jth reaction
F = Gibb's free energy
f' = ratio of local to freestream velocity (boundary layer)
$G^{\pm}$ = slopes of right and left running characteristics
g = ratio of local to freestream stagnation enthalpy (boundary layer)
H = stagnation enthalpy
h = enthalpy of mixture
h_i = enthalpy (including heat of formation), ith species
I = number of chemical species
k_i = catalytic wall recombination rate constant, ith atomic species
k_j^{eq} = equilibrium constant, jth reaction
k_j^f, k_j^r = forward and reverse reaction rate constants, jth reaction
N = number of chemical elements
Pr = Prandtl number
p = pressure
R = universal gas constant
Re = Reynolds number, based on freestream conditions
r = nozzle radius
S = entropy
s = distance along nozzle wall
T = temperature
t = time
U, V = velocity components in X and Y directions
u, v = velocity components in s and y directions
$\dot{w}_i$ = mass production rate per unit volume, ith species
$\bar{X}_i$ = moles of species i
X, Y = distance along and normal to axis of nozzle
y = distance normal to nozzle wall
z = local coordinate in direction of integration step, inviscid calculation
α_{ij}, β_{ij} = molar stoichiometric coefficients, ith species, jth reaction
β = pressure gradient parameter in boundary layer equations
β_0 = frozen expansion coefficient
δ = boundary-layer thickness
δ^* = displacement thickness
ζ = local coordinate along data line, inviscid calculation
η = transformed coordinate defined by Eq. (19)
θ = ratio of local to freestream temperature (boundary layer)
λ_j = progress variable, jth reaction
μ = viscosity
μ_i = chemical potential, ith species
ξ = transformed coordinate defined by Eq. (20)
ρ = density
σ_i, σ_n = ratio of local to freestream mass fraction, ith species, nth element (boundary layer)
ϕ_j = defined in Eq. (8)
ψ = stream function

Subscripts

e = freestream (edge of boundary layer)
i = chemical species
j = chemical reaction
n = element
w = wall
c = chamber conditions

Presented at the IAS 31st Annual Meeting, New York, January 21–23, 1963; revision received August 5, 1963. This research was partially funded by the U. S. Air Force through Arnold Engineering Development Center under Contract No. AF 40(600)-925.

* Staff Scientist, Space Science Laboratory. Member AIAA.
† Staff Scientist, Space Science Laboratory; now with Aerospace Corporation, San Bernardino, Calif. Associate Member AIAA.

I. Introduction

THREE types of flow, equilibrium, relaxing, and frozen, are encountered in the expansion of air from transonic to hypersonic speeds in the nozzle of a shock tunnel or an arc jet facility that provides a high-altitude environment at near-satellite velocities. In this paper, the flow is assumed to be in chemical equilibrium at the throat, with a high degree of dissociation. As shown by Bray[1] and Eschenroeder, Boyer, and Hall,[2] etc., as the gas expands downstream from the throat and is cooled, its composition tends to depart from equilibrium. The gas eventually "freezes," with a considerable fraction of the dissociated products remaining.

In such facilities, the extent of the usable inviscid core flow may be severely limited by boundary-layer growth. Any estimate of the boundary-layer development should include the influence of finite-rate chemical reactions. Because of the simplifications resulting when the boundary layer may be treated as either in equilibrium or frozen, it is important to establish when these conditions occur in nozzle boundary layers. It is expected that the increased density in the boundary layer, which is characteristic at transonic speeds with wall cooling, will maintain the boundary layer in equilibrium downstream of the throat as long as the core flow remains in equilibrium. However, far from the throat, where the core flow is frozen, heating caused by viscous dissipation will reduce the density in the boundary layer below freestream values and decrease atomic recombination rates. The boundary layer will be essentially frozen. It is in the intermediate Mach number range, in which the core flow is changing from equilibrium to frozen,

that solutions with coupled finite-rate chemical reactions must be carried out for the boundary layer.

II. Inviscid Flow Field

A. Basic Equations

The equations describing the flow in the inviscid flow regions were developed by Wood and Kirkwood,[5] assuming the fluid to be a mixture of perfect gases with chemical reactions taking place at arbitrary rates. Here, the additional assumption of local thermodynamic equilibrium (including vibrational equilibrium) is made, although this assumption is not essential to the analysis.

The chemical reactions can be written in the form

$$\sum_i \alpha_{ij}\tilde{X}_i \underset{k_j^r}{\overset{k_j^f}{\rightleftarrows}} \sum_i \beta_{ij}\tilde{X}_i \tag{1}$$

The progress variable λ_j for the jth reaction is now defined in terms of the net reaction rate r_j:

$$d\lambda_j/dt = r_j \tag{2}$$

The reaction rate r_j is the difference between the forward and reverse reaction rates for the particular reaction.

The production rate per unit volume of species k can be expressed in terms of the rate constants and the molar concentrations:

$$\dot{w}_k = m_k\Sigma_j(\alpha_{kj} - \beta_{kj}) \times [k_j^f\Pi_i(C_i\rho/m_i)^{\alpha_{ij}} - k_j^r\Pi_i(C_i\rho/m_i)^{\beta_{ij}}] \tag{3}$$

With the assumption of local thermodynamic equilibrium, the flow equations of Wood and Kirkwood are

$$(dp/dt) + \rho c_0^2\nabla\cdot\mathbf{U} = \rho c_0^2\Sigma_j\phi_j r_j \tag{4}$$

$$\rho(d\mathbf{U}/dt) = -\nabla p \tag{5}$$

$$T(dS/dt) = -\Sigma_j r_j\Delta_j F \tag{6}$$

where the derivative of ρ has been eliminated from the continuity equation by use of

$$c_0^2(d\rho/dt) = (dp/dt) - \rho c_0^2\,\Sigma_j\phi_j r_j \tag{7}$$

where

$$\phi_j = \rho[\Delta_j(1/\rho) - (\beta_0/C_p^0)\Delta_j h] \tag{8}$$

The operator Δ_j is defined in the equation

$$\nabla_j F \equiv (\partial F/\partial\lambda_j)_{T,p,\{\lambda\}_j} = \Sigma_i\mu_i\nu_i^j \tag{9}$$

where the subscripts T, p, $\{\lambda\}_j$ denote differentiation with T, p, and all the λ's except λ_j held constant. The equation of state is taken in the form

$$p = \rho RT\Sigma_i(C_i/m_i) \tag{10}$$

Equations (2 and 4–10) describe the inviscid flow field. These equations are integrated numerically,[4] using the equilibrium thermodynamics of Hochstim[11] and the reaction rates of Wray.[3]

B. Method of Solution

For supersonic speeds, the preceding equations have real characteristics. The equations of these characteristics in the (X,Y) coordinate system (Fig. 1) are

$$G^{\pm} = \left.\frac{dY}{dX}\right|_{\pm} = \frac{UV \pm c_0(U^2 + V^2 - c_0^2)^{1/2}}{U^2 - c_0^2} \tag{11}$$

and

$$dY/dX|_0 = V/U \tag{12}$$

since the streamlines are also characteristics. Note that the

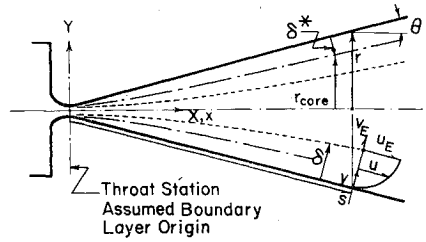

Fig. 1 Coordinate system.

appropriate speed of sound in these equations is the frozen speed of sound.[5]

The method of characteristics for a reacting gas is much more complicated than for a nonreacting gas. The reaction equations must be integrated along streamlines, and the pressure, say, must be matched with that obtained from an integration along the characteristics. In general, this involves an iteration.

In the integration procedure used here, the method of characteristics is not used (i.e., the equations are not integrated along characteristics). Instead, the characteristics are used to establish a local coordinate system in which the differential equations are replaced by finite difference equations. All properties are then integrated in a simple marching procedure along an approximation to the streamline. (The main advantage of this procedure is to reduce the necessary machine time for calculations.) As a result of this procedure, pressure pulses are propagated across the flow field along lines that are unrelated to the characteristics. Hence, care must be taken in using this method where waves are an important feature of the flow. Moreover, care must be taken to use sufficiently small spacing of points along a data line as well as a small step-size where gradients are large in the direction normal to the streamlines. This condition is likely to occur in flows over bodies.

The method is carried out in the following way: suppose that points 1 and 2 (Fig. 2) are points along an initial data line that is not a characteristic. The intersection of the proper characteristics from points 1 and 2 determines a new point, B. Point A is taken at the midpoint of the line segment (points 1 and 2). Conditions at A are found by linear interpolation between points 1 and 2.

A local coordinate system, $z(X,Y)$, $\zeta(X,Y)$, is then defined such that the line segment (points 1 and 2) is given by z = const, and the line segment (A,B) is given by ζ = const. This is not necessarily an orthogonal coordinate system. The flow equations are transformed to the system (z,ζ) and put into finite difference form:

$$\frac{\partial p}{\partial\zeta} = \frac{p_2 - p_1}{a} \qquad \frac{\partial p}{\partial z} = \frac{p_3 - p_A}{b}, \text{ etc.} \tag{13}$$

where point 3 is any desired point along the line (A,B). This allows the step size b to be made as small as desired without increasing the number of points along a data line. By evaluating the derivatives at A, the conditions at point 3 can be found immediately from the difference equations.

It should be noted that, in this procedure, the domain of dependence of the differential equations at point 3 lies within the domain of dependence of the difference equations, the line segment (points 1 and 2).

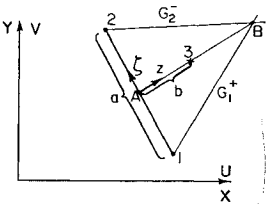

Fig. 2 Local coordinate system for finite difference equations of the inviscid core.

This procedure is repeated in a marching process, generating new data lines with each step. Points along the boundaries of the flow field are calculated with a modified procedure to account for the imposed boundary conditions.

C. Starting Procedure

The finite difference procedure outlined in the previous sections is started along a data line where the flow is in equilibrium. A perturbation procedure is necessary to depart from equilibrium in order to continue with finite-rate chemical calculations. In practice, this is done automatically. It may be seen from Eq. (3) that under equilibrium conditions the net species production rates are all zero. Hence, in the first step of the finite-rate calculation, the calculations are carried out with zero reaction rates. Since the temperature and pressure gradients are nonzero, the chemical composition is then out of equilibrium after the first step. Because of the fast reaction rates near equilibrium, the step size must be very small initially.

III. Boundary-Layer Formulation

A. Basic Equations

In addition to the effect of changing composition in the inviscid case, the chemical composition of the boundary layer will be influenced by the catalytic recombination of atoms at the wall and by the diffusion of atoms and molecules across the boundary layer (sublimation and chemically reacting surface effects are neglected), as well as by gas-phase reactions within the boundary layer. Diffusion velocities are determined by treating the dissociated air as an effective binary mixture of atoms and molecules, so that binary diffusion coefficients may be used. Temperature diffusion is neglected.

The basic formulation for the boundary layer solution is similar to that given by Fay and Riddell,[6] Lees,[7] and Scala,[8] except that the concept of local similarity is applied along the entire length of the surface, and five different chemical species are considered.

The general conservation equations for such a multicomponent gas with I chemical species and including the usual boundary-layer assumptions are as follows:

Over-All Continuity

$$(\rho ur)_s + (\rho vr)_y = 0 \tag{14}$$

Continuity of Species (Diffusion)

$$\rho(uC_{is} + vC_{iy}) - (\rho D_i C_{iy})_y = \dot{w}_i \qquad i = 1,2,\ldots;\ I-1 \tag{15}$$

Momentum

$$\rho(uu_s + vu_y) = -p_s + (\mu u_y)_y \tag{16}$$

Energy

$$\rho(uH_s + vH_y) = [(\mu/Pr)H_y]_y + \{\mu[1 - (1/Pr)]uu_y\}_y \times + \Sigma_i\{\rho D_i[1 - (1/L_i)]h_i c_{iy}\}_y \tag{17}$$

State

$$p = \rho TR\Sigma_i(C_i/m_i) \tag{18}$$

where $\Sigma_i C_i = 1$.

B. Similarity Considerations

The set of conservation and state equations comprises a system of algebraic and partial differential equations with independent variables s and y. They may be reduced to ordinary equations by a change of variables which makes use of the assumption of "local similarity." This assumption reduces s from a variable to a parameter, so that the boundary-layer profiles may be found independently at each station. Specification of an initial profile, then, is no longer necessary.

The transformation used by Fay and Riddell (Lees-Dorodnitsyn)is used here:

$$\eta = \frac{\rho_e u_e r}{(2\xi)^{1/2}} \int_0^y \frac{\rho}{\rho_e}\, dy \tag{19}$$

and

$$\xi = \int_0^s \rho_w \mu_w u_e r^2 ds \tag{20}$$

The introduction of the stream function ψ that satisfies the global continuity equation yields $\psi_y = \rho ru$ and $\psi_s = -\rho rv$. With the definition of f such that $f_\eta = u/u_e$, then $f = \psi/(2\xi)^{1/2}$, and

$$\rho rv = -(d/ds)\{(2\xi)^{1/2} f\} \tag{21}$$

With $g = H/H_e$, $\theta = T/T_e$, $\sigma_i = C_i/C_{ie}$, and $l = \rho\mu/\rho_w\mu_w$, the remaining conservation equations are

$$\left[\frac{l}{Pr}(L_i\sigma_{i\eta})\right]_\eta + f\sigma_{i\eta} + \frac{2\xi}{C_{ie}}\left(\frac{d\xi}{ds}\right)^{-1}\left[\frac{\dot{w}_i}{\rho u_e} - f_\eta\sigma_i\frac{dC_{ie}}{ds}\right] = R_i \qquad i = 1,2,\ldots,I-1 \tag{22}$$

$$(lf_{\eta\eta})_\eta + ff_{\eta\eta} + 2\xi\left(\frac{\rho_e}{\rho} - f_\eta^2\right)\frac{du_e/ds}{u_e}\left(\frac{d\xi}{ds}\right)^{-1} = R_m \tag{23}$$

$$\left(\frac{lg_\eta}{Pr}\right)_\eta + fg_\eta + \frac{u_e^2}{H_e}\left[\left(1 - \frac{1}{Pr}\right)lf_\eta f_{\eta\eta}\right]_\eta + \frac{l}{Pr}\left[\sum_i C_{ie}\frac{h_i}{H_e}(L_i - 1)\sigma_{i\eta}\right]_\eta = R_e \tag{24}$$

where the residues R_i, R_m, and R_e consist of the nonsimilar terms

$$R_i = 2\xi(f_\eta\sigma_{i\xi} - f_\xi\sigma_{i\eta})$$
$$R_m = 2\xi(f_\eta f_{\eta\xi} - f_\xi f_{\eta\eta})$$
$$R_e = 2\xi(f_\eta g_\xi - f_\xi g_\eta)$$

The local similarity assumption requires that these residues be negligible, and the quantities f, g, and σ_i are then integrated as functions of η only.

The assumption of local similarity has been shown by Moore[17] to be justified for Eqs. (23) and (24) under the condition of hypersonic flow and a cold wall, provided that β is small ($\beta < 0.25$). In Eq. (22), R_i will be negligible if the third term on the left side of the equation is small, at least over most of the boundary layer. At the wall, f_n vanishes. For a cold wall, ρ is relatively large, and $\dot{w}_i$ is small. At the edge of the boundary layer, $f_n \to 1$, $\sigma_i \to 1$, and

$$\dot{w}_i/\rho|_{\eta\to\infty} = U_e(dC_{ie}/ds)$$

Hence the term vanishes in the freestream and is small at the wall. However, since the reaction rates through the boundary layer can vary over a large range depending on the particular reactions involved, the species concentrations, and the local temperature and density, no general statements can be made about the size of this term. As a result, the use of the local similarity assumption must be justified a posteriori.

As shown by Lees, it will prove convenient to replace $N - 1$ of the continuity of species equations by continuity equations for the *element* mass fractions (N elements), because the chemical source term, $\dot{w}_n$, for each element n must vanish in any chemical reaction. The normalized mass fraction of each element $\sigma_n = C_n/C_{ne}$ is found from the species mass fractions:

$$\sigma_n C_{ne} = \sum m_{ni} C_{ie}\sigma_i \qquad n = 1,2,\ldots,N \tag{25a}$$

where

$$\sum_{n=1}^{N} \sigma_n C_{n_e} = 1 \tag{25b}$$

and where the m_{ni} are the mass fraction of element n in species i. Multiplying each of Eqs. (22) by the appropriate m_{ni} and summing over all species gives the required diffusion equations:

$$[(l/Pr)(L_n\sigma_n)_\eta]_\eta + f\sigma_{n\eta} = 0 \qquad n = 1, 2, \ldots, N-1 \tag{26}$$

where L_n is the mean Lewis number for the element n and varies with composition if the Lewis numbers are not identical for all chemical species.

In summary, Eqs. (22–26) and Eq. (18) form a system of $N + I + 3$ algebraic and ordinary differential equations. The independent variable is η, and the dependent variables are the N normalized element mass fractions σ_n, the I normalized species mass fractions σ_i, the velocity function f, the enthalpy ratio g, and the density ρ.

The functions l, Pr, L_i, L_n, and h_i are, in general, functions of temperature and, except for h_i, dependent upon mixture ratio. In principle, these functions may be evaluated at each point in the boundary layer based on the local temperature and composition, e.g., Scala and Baulknight.[12] However, this degree of sophistication does not appear warranted for the illustrative problems, since, for anything more than a binary mixture, the computation of the transport coefficients is somewhat approximate, and the added complexity is difficult to justify, e.g., Lighthill.[13] Here Pr and L_i are taken as constants. The viscosity μ that enters in l is based on the Sutherland law as a function of temperature only.

C. Boundary Conditions

The set of Eqs. (22–26) is of order $5 + 2(I - 1)$, and this number of boundary conditions is required to effect a solution. The system is of the two-point or split boundary-value type, since some of the boundary conditions are given in the inviscid stream and others at the wall. In the inviscid stream, $\eta = \infty$, $2 + (I - 1)$ boundary conditions are specified, viz.,

$$f_\eta = 1 \qquad g = 1 \qquad \sigma_i = 1 \quad (i = 1, 2, \ldots I - N) \qquad \sigma_n = 1 \quad (n = 1,2, \ldots N - 1) \tag{27}$$

At the wall $\eta = 0$, several different sets of boundary conditions may be imposed, depending upon the chemical and physical properties of the surface. The mass flux per unit area for a given species normal to the surface is

$$(\rho v)_i = C_i(\rho v) - \rho D_i C_{i_y}$$

where the first term on the right represents the mass flux carried by the mean flow, and the second term is that carried by diffusion. At a solid noncatalytic surface both $(\rho v)_w$ and $(\rho v)_{iw}$ must vanish. However, with catalytic wall effects, $(\rho v)_{iw}$ for an atomic species consists of the mass flux recombining at the surface by catalytic action. For a cold wall, the strength of this catalytic surface sink is given by $-\rho_w k_i C_{iw}$, where k_i is the catalytic recombination rate constant for the ith atomic species and has the dimension of velocity. Thus, for an atomic species, the wall boundary condition becomes $k_i C_{iw} = D_{iw} C_{iy_w}$, which, in terms of the transformed coordinates, gives

$$\sigma_{i\eta w} = \frac{(2\xi)^{1/2}}{r\mu_w} \frac{Pr}{L_i} \frac{k_i}{u_e} \sigma_{iw} \tag{28a}$$

and the wall derivative is proportional to the catalytic rate constant k_i. For the molecular species (primed), the wall boundary condition is

$$\sigma_{i\eta w}' = -\frac{(2\xi)^{1/2}}{r\mu_w} \frac{Pr}{L'} \frac{k_i C_{iw}}{u_e C_{iw}'} \sigma_{iw}' \tag{28b}$$

where the catalytic rate constant k_i is that for the corresponding atomic species C_i; $\sigma_{i\eta w}'$ vanishes for molecular species unaffected by wall catalysis.

The *element* mass fractions are of course not influenced by wall catalysis, and the corresponding boundary condition becomes

$$(L_n\sigma_n)_{\eta w} = 0 \tag{28c}$$

With wall suction, these boundary conditions remain unchanged provided that the mass flux of each species being sucked through the surface is proportional to the concentration of that species at the surface.

Equations (28a) and (28b) provide $I - N$ wall boundary conditions, and Eq. (28c) provides an additional $N - 1$. The remaining three of the required $3 + (I - 1)$ wall boundary conditions are supplied by the wall values of f, f_n, and g. The initial value of f is found from the integral of Eq. (21):

$$f_w = -\frac{1}{(2\xi)^{1/2}} \int_0^s \rho_w v_w r ds \tag{29}$$

which vanishes for the nonsuction case. The nonslip condition at the surface gives $f_\eta = 0$, whereas the specification of the surface temperature is required to provide the final boundary condition.

D. Method of Solution

Equations (18 and 22–27), together with boundary conditions (27–29), etc., are to be solved for f, g, ρ, σ_i, and σ_n. Because of the nonlinearity of the system and because of the split boundary conditions, no direct integration procedure exists by which closed-form solutions may be obtained.

The general procedure for obtaining a solution is to integrate Eq. (22) for $I - N$ of the chemical mass fractions σ_i. Equation (26) is then integrated for $N - 1$ of the element mass fractions σ_n. The remaining σ_n is found from the conservation principle, Eq. (25b), whereas the remaining σ_i's are obtained from the simultaneous solution of Eq. (25a).

A forward integration procedure is employed whereby the unknown mass fractions and derivatives at the wall are assumed. The number of these unknown parameters that are independent is $2 + (I - 1)$, viz., $f_{\eta\eta}, g_\eta, \sigma_i$, $i = 1,2, \ldots I - N$, and σ_n, $n = 1,2, \ldots N - 1$. The remaining mass fractions are then given by Eqs. (25), following which all of the wall boundary conditions are readily evaluated. The integration is then carried out numerically from the wall into the freestream, and the $2 + (I - 1)$ freestream boundary conditions are evaluated and compared with the values prescribed by Eqs. (27). In practice, a finite value is used for the freestream (e.g., $\eta_e = 4$). A perturbation procedure in the unknown parameters is then carried out to obtain an improved solution that provides a better match of the freestream boundary conditions. It is, of course, required that all derivatives vanish at η_e. If this is not the case, the matching of the freestream boundary conditions must be carried out at a larger value of η_e.

The success of the method is dependent upon the closeness of the assumed solution and upon the linearity of the deviations in the freestream values with the perturbations of the assumed parameters. Based on this linear dependence, an interpolation procedure is employed which corrects the assumed solution. Additional improved solutions are then obtained by a matrix modification procedure as outlined by Kulakowski and Stancil.[15]

To simplify the method as much as possible, it is necessary to minimize the number of unknown parameters at the wall. This may be accomplished for many practical problems by decoupling some of the equations from the remainder of the system. In particular, if the Lewis numbers of all the chemical species are the same, $L_i = L$, then the element Lewis numbers are constant, $L_n = L$, and examination of Eq. (28c) indicates that $\sigma_{n_{\eta w}} = 0$. The solutions of the

Table I Chemical reactions considered in calculations

1	$O_2 + M \rightleftarrows 2\,O + M$
2	$N_2 + M \rightleftarrows 2\,N + M$
3	$NO + M \rightleftarrows N + O + M$
4	$NO + O \rightleftarrows O_2 + N$
5	$N_2 + O \rightleftarrows NO + N$

corresponding diffusion equations, Eq. (26), are now simply $\sigma_n = 1$, $n = 1,2, \ldots N-1$, and the order to the parametric system is reduced by $N-1$.

The momentum equation, Eq. (23), will decouple only if the velocity gradient term vanishes and the ratio l is held constant. With $l = 1$, this becomes the Blasius equation, and $f_{\eta\eta w} = 0.47$. For any other value of l, it is readily shown that the solution is $f = l^{1/2} f_B(\eta/l^{1/2})$, where f_B is the Blasius solution. Although approximate solutions may be found by using an average l based on the Sutherland viscosity law similar to the Chapman and Rubesin constant C,[16] the large gradients in a hypersonic nozzle will still prevent the uncoupling of Eq. (23) for most practical nozzle calculations.

Similarly, Eq. (24), the energy equation, may be decoupled from the diffusion equations under the somewhat restrictive assumptions $Pr = L = 1$, $l = \text{const}$, and zero velocity gradient. Taking $g_B(\eta)$ as the solution to the simplified energy equation with $l = 1$,

$$g_B = (1 - g_w) f_{B_\eta} + g_w$$

For $l \neq 1$,

$$g = l^{1/2}(1 - g_w) f_{B_\eta}(\eta/l^{1/2}) + g_w$$

Finally, some discussion of the diffusion or continuity of species equations, Eqs. (22), is warranted. It is well known that, with the simplifying assumptions of $Pr = L = 1$, frozen gas phase reactions ($\dot{w}_i = 0$), and zero freestream gradients, the energy and diffusion equations are similar, and the solutions $g(\eta)$ and $\sigma_i(\eta)$ differ only because of the wall boundary condition.

The third term from the left with $\dot{w}_i$ and dC_{i_e}/ds contains the effects of gas-phase chemical reactions. The size of this reaction term indicates the ratio of the residence time in the boundary layer to the time required to restore the freestream composition. A large residence time corresponding to a long

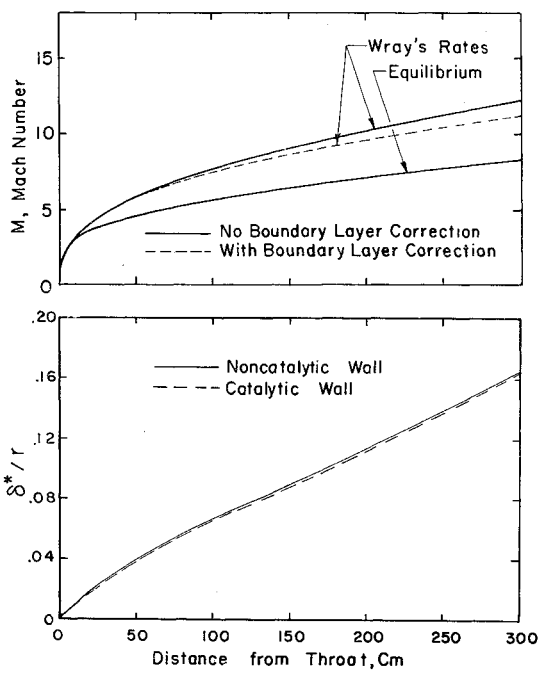

Fig. 3 Calculated displacement thickness and Mach number, General Dynamics CHST facility.

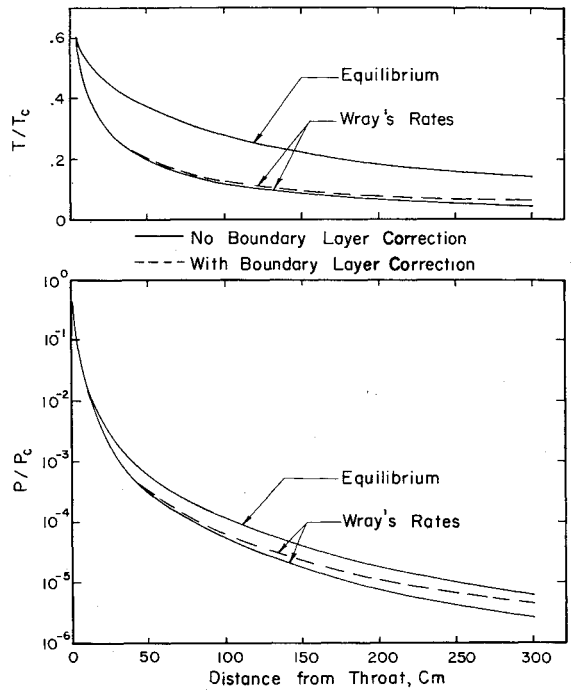

Fig. 4 Calculated static pressure and freestream temperature, General Dynamics HCST facility.

wall length, or a small chemical time resulting from fast reaction rates or a small freestream concentration, will magnify the size of this highly nonlinear reaction term. The limiting solution for equilibrium flow is approached as this term becomes infinitely large. When this occurs, the diffusion equation is no longer applicable, as pointed out in the Introduction.

This term may be very large for the minor chemical species that are present in the freestream in only trace amounts, and the subsequent solutions of the diffusion equation for these species will become highly sensitive to small changes in the concentrations of the other species. Since only $I - N$ of the I possible diffusion equations must be integrated, the choice should be based on the most important species. An alternate approach is to neglect the minor species entirely in the solution of the coupled boundary-layer equations. The solution for the minor species in the boundary layer, if desired, is then obtained by subsequently integrating the decoupled diffusion equations for these species with all other boundary layer properties remaining unchanged. This approach is obviously not recommended for cases where trace species play a large role in the chemical reactions, as in hydrogen-oxygen reactions.

IV. Sample Calculations

Sample calculations were made for the flow of chemically reacting air in the conical nozzle of the General Dynamics/Convair hypersonic shock tunnel (CHST). Pertinent nozzle dimensions are a length of 308 cm and a $6\frac{1}{3}°$ semivertex angle.[18] The calculations were made for the 0.45-in.-diam throat (1.143 cm). Reservoir conditions were $p_c = 82$ atm and $T_c = 6667°$K. The chemical reactions considered in the calculations are listed in Table 1.

A quasi-one-dimensional inviscid flow calculation, assuming thermodynamic and chemical equilibrium, was made to obtain conditions at the throat and along the starting supersonic data line for the finite rate inviscid calculations. The resulting equilibrium Mach number, static pressure, temperature, and chemical species concentrations are shown in Figs. 3–5.

The finite-rate inviscid core calculations were initiated approximately 0.2 cm downstream from the throat, where

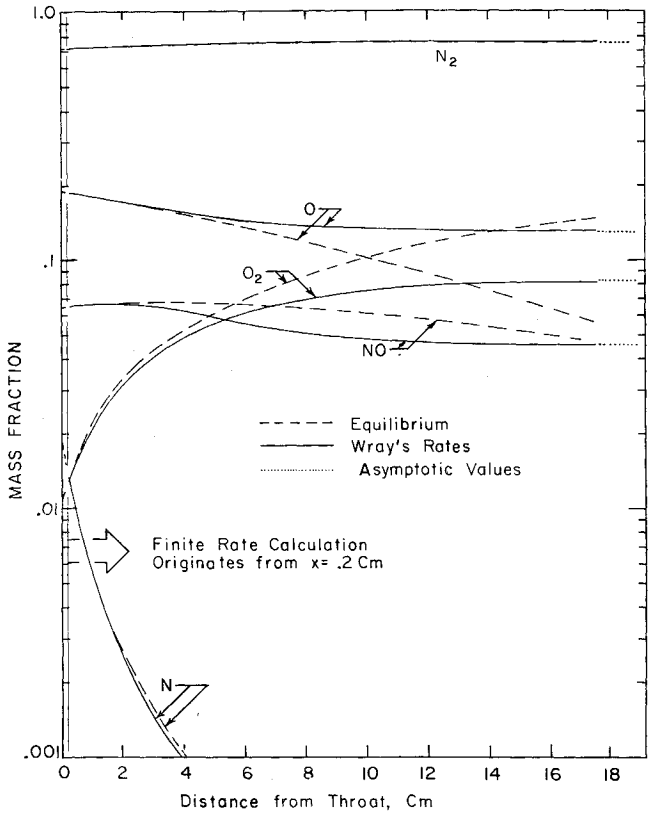

Fig. 5 Calculated chemical composition in the inviscid core, General Dynamics CHST facility.

the frozen Mach number had a value of 1.2. Because of the conical geometry of the nozzle, point source type of flow was assumed. The inviscid finite rate calculations were then carried out on the IBM 7090 computer by the difference procedure described in Sec. II. The results are given in Figs. 3–5 and compared with the equilibrium values. These results are in qualitative agreement with the results of Eschenroeder, Boyer, and Hall,[2] although different reservoir conditions and throat contours prevent direct comparison.

The finite-rate solution departs from equilibrium about 1 cm from the throat and is essentially frozen (constant composition) at 20 cm from the throat. It is of interest that the equilibrium and finite-rate solutions are essentially identical for a distance of about 1 cm downstream from the initial data line and then depart smoothly, indicating that the assumption of equilibrium near the throat was justified. Extraordinarily small step sizes (0.0014 cm) were required to prevent the finite-rate solution from diverging when the flow was near equilibrium. The step size, of course, increases with Mach number.

The boundary-layer solution was found by numerically integrating the boundary layer equations on the IBM 7090 computer as outlined in Sec. III. Wray's chemical reaction rates were used. A constant wall temperature $T_w = 317°K$ was assumed, and both catalytic and noncatalytic wall cases were treated. For the catalytic wall case, the catalytic recombination rate was taken as 10^4 cm/sec for oxygen and nitrogen atoms. This corresponds to nearly complete recombination of the incident atoms.[11] The NO species was assumed to be unaffected by wall catalysis.

The boundary-layer equations were integrated at 10, 50, 100, 150, 250, and 308 cm from the throat. The displacement thickness was evaluated, and the location of the profile and corresponding inviscid core conditions was then displaced downstream to provide a constant mass flow (Fig. 3). The boundary layer has only a negligible effect on the chemistry in the core because the boundary displacement thickness is an appreciable fraction of the nozzle radius only

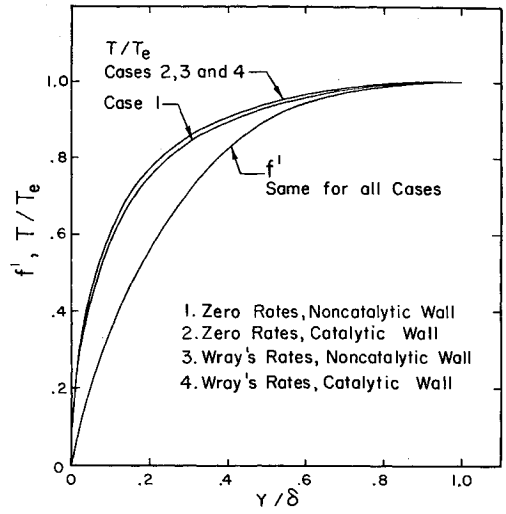

Fig. 6 Calculated boundary-layer velocity and temperature profiles, 10 cm from throat, General Dynamics CHST facility.

after the core composition has frozen ($\delta^*/r \doteq 0.01$ at $X = 20$ cm).

The corresponding pressure and temperature variation in the nozzle core, including boundary-layer displacement effects, are given in Fig. 4. The chemical composition is identical to that without boundary-layer effects (Fig. 5).

Calculated velocity, temperature, and species profiles in the boundary layer at the 10-cm station are shown in Figs. 6 and 7. Results are presented for four cases: 1) zero rates (frozen) and a noncatalytic wall, 2) zero rates with a catalytic wall, 3) Wray's rates, noncatalytic wall, and 4) Wray's rates with a catalytic wall. The cases with frozen chemistry were included for comparison. It is clear from the figures that the gas-phase reactions reduce the concentration of the atomic species O and increase that of the molecular species O_2 and NO in the boundary layer. The distribution of N was not found, since N is present in the freestream in only trace amounts, i.e., $C_{N_e} = 10^{-4}$, at this station. For the catalytic wall cases, the effect of the gas-phase chemical reactions is much less, because the catalytic recombination occurring at the wall drives the flow toward

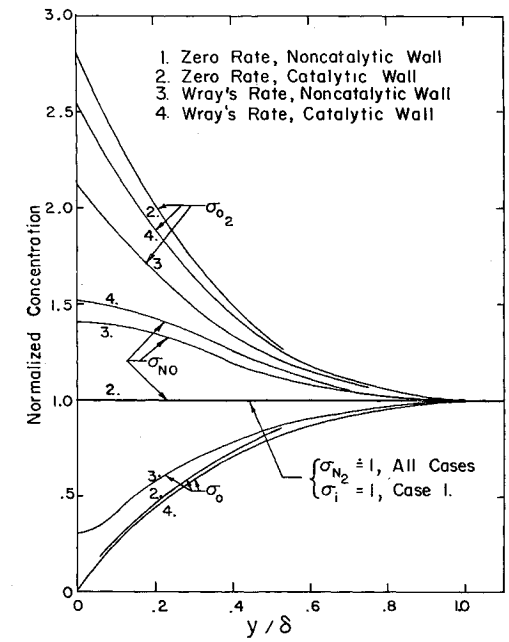

Fig. 7 Calculated boundary-layer chemical species profiles, 10 cm from throat, General Dynamics CHST facility.

Table 2 Calculated boundary-layer properties, 10 cm from throat, General Dynamics CHST facility

Assumpton	δ, cm	δ^*, cm	$f_{\eta\eta}(0)$	$g_\eta(0)$	C_f	C_h
Zero rates, noncatalytic wall	0.057	0.0091	0.437	0.231	0.00121	0.000522
Wray's rates, noncatalytic wall	0.057	0.0081	0.427	0.272	0.00122	0.000576
Zero rates, catalytic wall	0.056	0.0074	0.420	0.272	0.00123	0.000576
Wray's rates, catalytic wall	0.057	0.0074	0.418	0.272	0.00122	0.000576

Table 3 Calculated boundary-layer properties, 50 cm from throat, General Dynamics CHST facility

Assumption	δ, cm	δ^*, cm	$f_{\eta\eta}(0)$	$g_\eta(0)$	C_f	C_h
Zero rates, noncatalytic wall	0.57	0.19	0.56	0.26	0.00126	0.00046
Wray's rates, noncatalytic wall	0.57	0.19	0.56	0.26	0.00125	0.00046
Zero rates, catalytic wall	0.57	0.18	0.54	0.30	0.00127	0.00051
Wray's rates, catalytic wall	0.57	0.18	0.54	0.30	0.00127	0.00051

the equilibrium composition and reduces the net reaction rates. In fact, the temperature profiles for cases 2, 3, and 4 are coincident, as shown in Fig. 6. The velocity profiles are identical for all cases, indicating that the coupling of the momentum equation to the remainder of the system is weak.

Table 2 lists some additional boundary layer properties at the 10-cm station. The gas-phase reactions reduce the displacement thickness by 10% and increase the Stanton number C_h by the same percentage for the noncatalytic wall case. Changing from a noncatalytic to catalytic wall without gas-phase reactions decreases δ^* by nearly 20% but produces no further increase in C_h. Introducing gas-phase reactions with the catalytic wall produced no additional changes in δ^* or C_h, again demonstrating the negligible effect of the gas-phase reactions with a catalytic wall. The variation in local skin friction coefficient C_f shown in Table 2 is small and within the accuracy of the calculations.

Similar data for the 50-cm station are presented in Figs. 8 and 9 and in Table 3. The core flow at this station is frozen, and it is interesting to determine the effects of gas-phase reactions on the boundary layer. At the 10-cm station, where the core flow was not frozen, gas-phase reactions had an appreciable effect for the noncatalytic wall case only. At the 50-cm station, the effect is negligible even for the noncatalytic wall case. Thus, finite-rate chemical reactions need not be considered in the boundary-layer calculations further downstream than the 50-cm station.

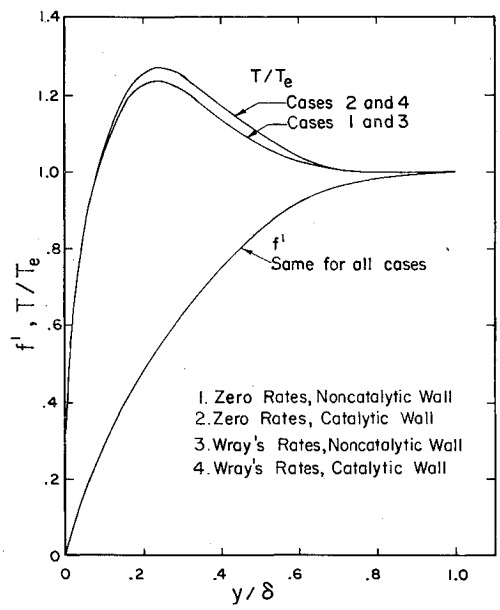

Fig. 8 Calculated boundary-layer velocity and temperature profiles, 50 cm from throat, General Dynamics CHST facility.

Even at this distance, where the core flow and boundary layer have frozen gas-phase reactions, the displacement thickness is less than 3% of the local nozzle radius. Thus, when finite-rate chemical reactions are important in the boundary layer, the boundary layer is still too thin to influence the development of the inviscid core flow. The generalization of this result to other nozzle geometries and reservoir conditions appears reasonable, since, at the low densities for which boundary layers become thick, chemical reactions tend to be frozen.

Boundary-layer profiles at stations further downstream than 100 cm have been compared on the basis of wall catalysis only. The displacement thickness is shown in Fig. 3. It is of interest that wall catalysis has only a small influence on displacement thickness when the boundary layer becomes thick enough to influence the inviscid flow.

V. Concluding Remarks

Methods have been demonstrated for computing the inviscid flow and laminar boundary-layer development in hypersonic flows with finite-rate chemical reactions. The inviscid flow was found by a finite-difference procedure based on the method of characteristics. The boundary-layer equations were integrated with coupled chemical reactions by using the assumption of "local similarity."

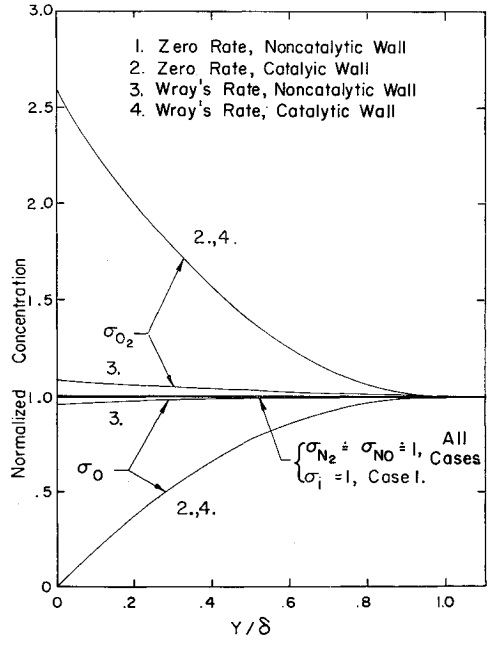

Fig. 9 Calculated boundary-layer chemical species profiles, 50 cm from throat, General Dynamics CHST facility.

Sample calculations were presented for the expansion of chemically reacting air in the General Dynamics CHST facility at prescribed reservoir conditions. Previous calculations for nonreacting nitrogen flows established the validity of the assumption of local similarity for low density conical flows for which experimental measurements were available.[19] The calculations with reacting air have demonstrated the following results:

1) The boundary layer has a negligible effect on the chemistry in the inviscid core.

2) Finite-rate gas-phase reactions have a significant influence on the boundary-layer properties only when the wall is noncatalytic.

3) Even with a noncatalytic wall, gas-phase reactions freeze in the boundary layer shortly downstream of where freezing occurs in the inviscid core. At this location, the boundary layer is still too thin to influence the core flow.

The application of these results to nozzle flows with other geometries and reservoir conditions remains to be demonstrated. However, this generalization appears reasonable because the low densities required to produce thick boundary layers also cause the chemical reactions in air to freeze.

References

[1] Bray, K., "Atomic recombination in a hypersonic wind tunnel nozzle," J. Fluid Mech. **6**, 1–32 (1959).

[2] Eschenroeder, A., Boyer, D., and Hall, J., "Exact solutions for non-equilibrium expansions of air with coupled chemical reactions," Cornell Aeronaut. Lab. AFOSR 622 (May 1961).

[3] Wray, K. L., "Chemical kinetics of high temperature air," *ARS Progress in Astronautics and Rocketry: Hypersonic Flow Research*, edited by F. R. Riddell (Academic Press, New York, 1962), Vol. 7, pp. 181–204.

[4] Schainblatt, A. H., "Numerical calculation of chemically reacting hypersonic flow fields," General Dynamics/Convair Rept. ZPh-109 (June 30, 1961).

[5] Wood, W. W. and Kirkwood, J. G., "Hydrodynamics of a reacting and relaxing fluid," J. Appl. Phys. **28**, 395–398 (1957).

[6] Fay, J. and Riddell, F., "Theory of stagnation point heat transfer in dissociated air," J. Aerospace Sci. **25**, 73–85 (1958).

[7] Lees, L., "Convective heat transfer with mass addition and chemical reactions," *Combustion and Propulsion, Third AGARD Colloquim* (Pergamon Press, Oxford, March 1958), pp. 451–498.

[8] Scala, S. M., "Hypersonic stagnation point heat transfer to surfaces having finite catalytic efficiency," *Proceedings of the Third U. S. National Congress of Applied Mechanics* (American Society of Mechanical Engineers, New York, 1958), pp. 799–806.

[9] Chung, P. M. and Anderson, A. D., "Heat transfer to surfaces of finite catalytic activity in frozen dissociated hypersonic flow," NASA TN D-350 (January 1961).

[10] Goulard, R., "On catalytic recombination rates in hypersonic stagnation heat transfer," Jet Propulsion **28**, 737–745 (1958).

[11] Hochstim, A. R., "Approximations to high-temperature thermodynamics of air in closed form," *Kinetics, Equilibria and Performance of High Temperature Systems, Proceedings of the First Conference*, edited by G. S. Bahn and E. E. Zukoski (Butterworth and Co. Ltd., London, 1960), pp. 39–52.

[12] Scala, S. M. and Baulknight, C. W., "Transport and thermodynamic properties in a hypersonic laminar boundary layer. Part I. Properties of the pure species," ARS J. **29**, 39–45 (1959).

[13] Lighthill, M. J., "Dynamics of a dissociating gas. Part 2. Quasi-equilibrium transfer theory," J. Fluid Mech. **8**, 161–182 (1960).

[14] "JANAF thermochemical data," Dow Chemical Co., Thermal Lab., Midland, Mich. (December 1960).

[15] Kulakowski, L. J. and Stancil, R. T; "Rocket boost trajectories for maximum burnout velocity," ARS J. **30**, 612–618 (1960).

[16] Chapman, D. R. and Rubesin, M. W., "Temperature and velocity profiles in the compressible laminar boundary layer with arbitrary distribution of surface temperature," J. Aeronaut. Sci. **16**, 547–565 (1949).

[17] Moore, F. K., "On local flat-plate similarity in the hypersonic boundary layer," Cornell Aeronaut. Lab. Rept. AF-1285-A-2 (June 1960).

[18] Baltakis, F. P., "Performance capability of hypersonics laboratory shock tunnel," General Dynamics/Convair Rept. GDC-62-49 (March 1962).

[19] Levinsky, E. S. and Brainerd, J. J., "Inviscid and viscous hypersonic nozzle flow with finite rate chemical reactions," Arnold Eng. Dev. Center Rept. AEDC-TDR-63-18 (January 1963).